Fundamental and high-order anapoles in all-dielectric metamaterials via Fano-Feshbach modes competition

Article (Accepted Version)

Fundamental and high-order anapoles in all-dielectric metamaterials via Fano-Feshbach modes competition

Juan Sebastian Totero Gongora, Gael Favraud and Andrea Fratalocchi[†]

PRIMALIGHT, King Abdullah University of Science and Technology (KAUST), Thuwal 23955-6900, Saudi Arabia

E-mail: [†]andrea.fratalocchi@kaust.edu.sa

12[th] January, 2017

Abstract. One of the most fascinating possibilities enabled by metamaterials is the strong reduction of the electromagnetic scattering from nanostructures. In dielectric nanoparticles, the formation of a minimal scattering state at specific wavelengths, is associated with the excitation of photonic anapoles, which represent a peculiar type of radiationless state and whose existence has been demonstrated experimentally. In this work, we investigate the formation of anapole states in generic dielectric structures by applying a Fano-Feshbach projection scheme, a general technique widely used in the study of quantum mechanical open systems. By expressing the total scattering from the structure in terms of an orthogonal set of internal and external modes, defined in the interior and in the exterior of the dielectric structure, respectively, we show how anapole states are the result of a complex interaction among the resonances of the system and the surrounding environment. We apply our approach to a circular resonator, where we observe the formation of higher-order anapole states, which are originated by the superposition of several internal resonances of the system.

Submitted to: *Nanotechnology*

1. Introduction

It is well known that metamaterial structures can sustain states of minimal scattering under specific combinations of geometrical and materials configurations [1, 2, 3, 4]. Scattering-free nanostructures play a relevant role in a pletoria of applications, ranging from near-field sensing to energy harvesting and integrated coherent sources [5, 6]. However, the mechanism underlying the strong reduction of the scattered field is still a subject of debate, in particular when considering all-dielectric nanostructures [3, 2, 7, 8]. Recently, researchers have experimentally demonstrated that invisibility states in dielectric nanoparticles, occurring at specific wavelengths, are associated with the excitation of photonic anapole modes [9]. Anapoles, which manifest as non-radiating distributions of electromagnetic currents, appear in many different branches of physics, ranging from condensed matter to cosmology, where they have been

proposed as a possible candidate to explain the elusive dark matter [10, 11, 12, 13]. In photonic systems, anapole states originate from specific combinations of multipolar components that cancel each other in the far-field [14, 15]. As a consequence, the radiation pattern of an anapole mode is composed of purely evanescent waves and it is entirely confined in the near-field, where it can be exploited to amplify light-matter interactions [16, 17, 18]. In spherical and cylindrical structures, anapole modes arise naturally from the multipole decomposition of the electromagnetic fields, allowing for a convenient determination of the scattering suppression conditions [9, 10]. In a generic structure, conversely, the definition of internal modes is a challenging task, as generic dielectric resonators constitute open cavities that do not support a set of standard orthogonal modes [19, 20, 21, 22]. Nevertheless, non-conventional cavity systems, such as chaotic resonators or disordered structures, possess unique localization and energy harvesting properties, which can be exploited to develop novel applications at the nanoscale [23, 24, 25].

In this work, we take inspiration from the field of open quantum systems to develop a novel approach to the description of radiation-less states in dielectric structures [26, 27, 28, 29]. By resorting to a Fano-Feshbach partitioning scheme, we derive two complete sets of internal and external eigenmodes, whose mutual interaction is ruled by coupling terms defined on the resonator boundary and which allow to describe the electromagnetic scattering from the resonator in a rigorous fashion. With this general approach, which we derived directly from Maxwell's equations, we investigate the scattering suppression conditions for the system. Finally, in the case of a circular cavity, we identify higher-order anapole modes originated from the mutual competition of several internal resonances of the system and which can not be explained in terms of fundamental anapole modes.

2. Theoretical Methods

We begin our theoretical analysis by considering a generic dielectric cavity delimited by a boundary $\partial\mathcal{R}$, whose optical properties are expressed by a dielectric function $\varepsilon(\mathbf{x})$. The definition of the resonator boundary is completely general: it can either represent the boundary of a complex dielectric object, or a region containing several dielectric objects (see Fig. 1). The evolution of the electric field $\mathbf{E}(\mathbf{x}, t)$ follows Maxwell's wave equation, which reads:

$$\left[\nabla \times \nabla \times + \frac{\varepsilon(\mathbf{x})}{c^2}\partial_t^2\right]\mathbf{E}(\mathbf{x}, t) = 0. \tag{1}$$

A common way to study Eq. (1) is by introducing a set resonance modes $\psi(\mathbf{x})$ of the photonic cavity. The latter are defined as the solutions of the Helmholtz eigenproblem associated to Eq. (1), which reads:

$$\mathcal{L}|\psi\rangle = \frac{\varepsilon(\mathbf{x})\Omega^2}{c^2}|\psi\rangle, \tag{2}$$

where we introduced the differential operator $\mathcal{L} = \nabla\times\nabla\times$ and its eigenvalues Ω. In the following, we employ the bra-ket notation $|\psi\rangle = \psi(\mathbf{x})$ to achieve a compact notation. Whenever a complete set of eigenmodes for Eq. (2) can be obtained, the eigenbasis $|\psi\rangle$ can be employed to expand all the electromagnetic quantities of the system. By definition, however, a dielectric resonator is an open cavity and, therefore, it is not possible to define a set of orthogonal eigenmodes [20]. Historically, the definition of a set of orthogonal cavity modes for an open system has been subject of great theoretical

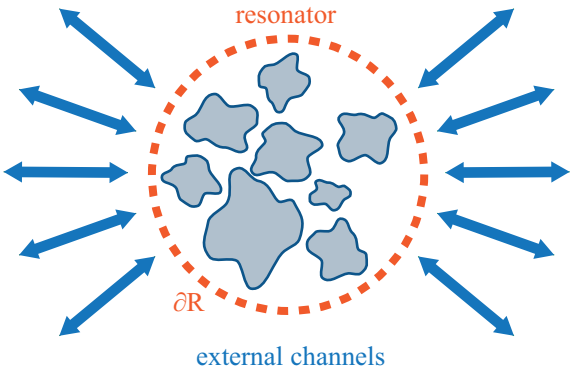

Figure 1. System configuration. The choice of the boundary $\partial\mathcal{R}$ is not fixed, and it can chosen as the boundary of a region containing all the dielectric objects composing the resonator.

efforts, as its implications range from quantum mechanical scattering to particle physics and quantum optics [19, 21, 22]. We address this problem by employing a Fano-Feschbach partitioning scheme, which allows to split all the electromagnetic quantities into 'resonator' and 'environment' contributions, with the only condition that all the projection components preserve their Hermiticity properties [27, 30, 28, 31]. Following the mathematical partitioning of the eigenspace from Eq. (2), the system can be expanded in terms of a set of internal $|\mu\rangle$ and external $|\nu\rangle$ eigenmodes, defined as the solution of the following independent eigenproblems:

$$\begin{aligned}\nabla\times\nabla\times|\mu_m\rangle &= \frac{\omega_m^2}{c^2}\varepsilon|\mu_m\rangle,\\ \nabla\times\nabla\times|\nu_n(\omega)\rangle &= \frac{\omega^2}{c^2}\varepsilon|\nu_n(\omega)\rangle,\end{aligned} \tag{3}$$

with the following boundary conditions:

$$\begin{aligned}\mathbf{n}\times\nabla\times|\mu_m\rangle|_{\partial\mathcal{R}} &= 0,\\ \mathbf{n}\times|\nu_n\rangle|_{\partial\mathcal{R}} &= 0,\end{aligned} \tag{4}$$

being $\mathbf{n}$ the normal unit vector to the surface $\partial\mathcal{R}$. Due to their definition, the internal and external eigenmodes are mutually orthogonal, and they form a complete set of eigenmodes for the resonator and for the environment subspaces, separately. Therefore, they coincide with the closed-cavity modes of the system, which describe the system in the absence of any interaction between the resonator and the external environment. In the realistic case of an open cavity, conversely, the Fano-Feshbach eigenmodes $|\mu\rangle$ and $|\nu\rangle$ are connected by *ad hoc* coupling terms, rigorously defined on the resonator boundary, which rule the resonant interaction between the internal and external eigenspaces. With this position, the evolution of the electromagnetic field in the interior of the resonator is described by introducing set of internal $\mathbf{A}(t) = \{a_1(t), a_2(t)\cdots a_m(t)\}$ and external $\mathbf{S} = \{s_1(t), s_2(t)\cdots s_n(t)\}$ modal operators, whose definition can be found in the Supplementary Information. In terms of the modal operators, the internal $\mathbf{E}_{int}(\mathbf{x}, t)$ and external $\mathbf{E}_{ext}(\mathbf{x}, t)$ electric fields are expressed

as:

$$\mathbf{E}_{int}(\mathbf{x},t) = \sum_m A_m(t)|\mu_m(\mathbf{x})\rangle, \tag{5}$$

$$\mathbf{E}_{ext}(\mathbf{x},t) = \int \mathrm{d}\omega \sum_n S_n(t,\omega)|\nu_n(\mathbf{x},\omega)\rangle. \tag{6}$$

After some lengthy but straightforward algebra, the evolution of the modal field amplitudes is dictated by the following set of dynamical equations:

$$\begin{aligned} \partial_t \mathbf{A}(t) &= j\boldsymbol{\Omega}\mathbf{A}(t) + \int \mathrm{d}\omega\, \boldsymbol{\mathcal{G}}(\omega)\mathbf{S}(\omega,t), \\ \mathbf{S}(\omega,t) &= \mathbf{S}^0(\omega,t) - \int_{t_0}^{t} \mathrm{d}\tau\, \boldsymbol{\mathcal{H}}(\omega)\mathbf{A}(\tau)e^{j\omega(t-\tau)}, \end{aligned} \tag{7}$$

where $\boldsymbol{\Omega} = \mathrm{diag}(\omega_1, \omega_2 \cdots \omega_N)$ is the resonance frequency matrix and $\mathcal{G}_{mn}(\omega)$ and $\mathcal{H}_{mn}(\omega)$ represent coupling terms defined on the boundary of the resonator. Eqs. (7) form a set of Fano-Feshbach Coupled-Mode equations (FF-CM), which provide a rigorous description of the dynamical evolution and mutual interaction of the internal and external modes of the system. In their current form, Eqs. (7) represent a multi-mode generalization of standard Time-Dependent Coupled-Mode Theory (TD-CM) equations, which are widely employed in the study of resonant photonic systems [32, 33, 34, 35]. More specifically, the FF-CM equations describe a set of impressed external sources $\mathbf{S}_0(\omega,t)$ which are coupled with a set of internal modes A_m by means of two frequency-dependent matrices $\boldsymbol{\mathcal{G}}(\omega)$ and $\boldsymbol{\mathcal{H}}(\omega)$. As can be easily verified by direct substitution, the coupling matrices introduced in Eqs. (7) fulfill all the symmetry properties of the standard equations from TD-CM (e.g. energy conservation and time-reversal invariance), as a direct consequence of the Hermiticity requirements of the Fano-Feshbach projection technique [22]. Differently from standard TD-CM approaches, which are based on a phenomenological description of the resonant interaction [36, 37], the coupling matrices and the resonant frequencies of the system can be directly computed from Maxwell's Eqs. (1). Such important difference opens to the realistic study of a large number of complex systems, such as chaotic or irregular shaped resonators and disordered many-body cavities. Moreover, as discussed in [38], the Fano-Feshbach approach can be easily extended to include complex light-matter interaction phenomena occurring in the interior of the resonator, such as stimulated emission of radiation or nonlinear material responses. Such possibility allows for a rigorous modeling of mode competition phenomena in non-conventional nanolasers characterized by strongly coupled multi-mode regimes.

3. Results and Discussion

3.1. Anapole generation condition

In a typical scattering experiment, the dielectric resonator is illuminated by an incident field $\mathbf{E}_{inc}(\mathbf{x},t)$, which constitutes the physical initial condition for the system, such as, e.g., a plane wave. The interaction with the resonator produces a scattered field $\mathbf{E}_{sca}(\mathbf{x},t) = \mathbf{E}_{ext}(\mathbf{x},t) - \mathbf{E}_{inc}(\mathbf{x},t)$, which is defined as the total variation of the external field due to the resonator. In the case of an open dielectric cavity, the total scattered field $\mathbf{E}_{sca}(\mathbf{x},t)$ is the result of two distinct mechanisms: the

resonant interaction with the cavity modes and the non-resonant reflection at the cavity boundary. The former is ruled by the dynamical equations (7), which can be solved in the Fourier domain ω and combined in a single equation for the external amplitudes $\mathbf{S}(\omega)$ obtaining:

$$\mathbf{S}(\omega) = \boldsymbol{\sigma}^A(\omega)\mathbf{S}^0(\omega), \tag{8}$$

where $\mathbf{S}^0(\omega)$ is the Fourier transform of $\mathbf{S}^0(\omega, t)$ and where we introduced the resonant scattering matrix $\boldsymbol{\sigma}_A(\omega)$, whose lengthy expression is included in the Supplementary Information.

The non-resonant reflections occurring at the cavity boundary, conversely, represent a fundamental property of the external modes and they are determined by the boundary conditions from Eqs. (4). In order to characterize the non-resonant interaction with the resonator, it is convenient to decompose the external eigenmodes $|\nu(\mathbf{x}, \omega')\rangle$ into ingoing $|\nu^+(\mathbf{x}, \omega')\rangle$ and outgoing $|\nu^-(\mathbf{x}, \omega')\rangle$ contributions as follows:

$$|\nu_n(\omega)\rangle = |\nu_n^+(\omega)\rangle + R_n^0(\omega)|\nu_n^-(\omega)\rangle, \tag{9}$$

with $R_n^0(\omega)$ a "reflection" coefficient, connecting the incoming and outgoing contributions, which can be determined by applying the boundary conditions from Eq. (4). In its current form, Eq. (9) allows for a straightforward interpretation, as it expresses the external modes in terms of an incoming contribution $|\nu_n^+\rangle$ and its reflection $R_n^0(\omega)|\nu_n^-(\omega)\rangle$ from the cavity boundary. Furthermore, such decomposition reflects the intuitive concept that, in order to constitute a complete basis for the total electromagnetic field in the external space, the environment eigenmodes are always expressed as a superposition of counter-propagating waves $|\nu_n^{(+)}(\omega)\rangle$ and $|\nu_n^{(-)}(\omega)\rangle$. As can be easily verified by applying the ortoghonality of the external eigenmodes to (9), the reflection coefficient is unitary: $(\mathbf{R}^0)^\dagger\mathbf{R}^0 = 1$ and, therefore, it can be rewritten as a pure phasor term as follows:

$$R_n^0(\omega) = e^{j\phi_n^0(\omega)}, \tag{10}$$

where $\phi_n^0(\omega)$ is commonly denoted as Fano coefficient. In terms of the ingoing and outgoing contributions, the incident field is expanded as follows:

$$\boldsymbol{E}_{inc} = \sum_n \lambda_n^+(\omega)|\nu_n^+(\omega)\rangle + \lambda_n^-(\omega)|\nu_n^-(\omega)\rangle, \tag{11}$$

where $\lambda_n^+(\omega)$ and $\lambda_n^-(\omega)$ are expansion coefficients which can be easily determined by projecting the incident field on the external eigenmodes. The expression for the total scattered field can be obtained by substituting Eqs. (5), (8) and (11) into the definition of the scattered field $\mathbf{E}_{sca}$, obtaining:

$$\mathbf{E}_{sca}(\mathbf{x}, \omega) = \sum_n \sigma_n^+(\omega)|\nu_n^+(\omega)\rangle + \sigma_n^-(\omega)|\nu_n^-(\omega)\rangle, \tag{12}$$

where the expressions for the ingoing and outgoing scattering coefficients $\sigma_n^{+,-}$ read:

$$\begin{aligned}\sigma_n^+(\omega) &= \sum_{n'} \sigma_{nn'}^A(\omega)S_{n'}^0(\omega) - \lambda_n^+(\omega),\\ \sigma_n^-(\omega) &= \sum_{n'} R_n^0(\omega)\sigma_{nn'}^A(\omega)S_{n'}^0(\omega) - \lambda_n^-(\omega).\end{aligned} \tag{13}$$

As expressed in Eq. (12), the total scattered field is composed of two contributions. Firstly, a set of ingoing contributions, ruled by the scattering coefficients $\sigma^+(\omega)$, which represent all the contributions that do not propagate away from the resonator space,

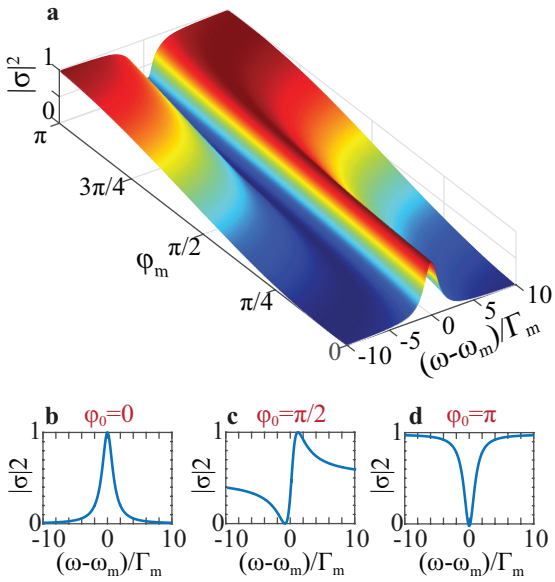

Figure 2. Anapole states . d-g Scattering suppression states in the case of an isolated resonance ω_0 as a function of the reflection phase $\phi_0(\omega)$. The interaction between the internal resonance and the external reflection $R_0 = e^{j\phi_0}$ produces the typical Fano-shaped profiles, ranging from purely lorentzian peaks (e, $\phi = 0$) to lorentzian dips (g, $\phi = \pi$). Due to the interaction with the slowly-varying background, the internal resonance produces a scattering suppression state for $\phi_0 \neq = 0$.

such as, e.g., all the evanescent and near-field contributions. Secondly, the outgoing scattering coefficients $\sigma^-(\omega)$, conversely, represent the measurable electromagnetic scattering from the cavity, which is composed of purely outgoing contributions [39]. The outgoing scattered field, which is the typical outcome of a scattering experiment, is then defined as:

$$\mathbf{E}_{out}(\mathbf{x},\omega) = \sum_n \sigma_m^-(\omega)|\nu_n^-(\omega)\rangle. \tag{14}$$

The condition for the formation of an anapole state corresponds to the situation where the amplitude of the outgoing scattering waves tend to a minimum, which implies a negligible measurable scattering in the dynamics. In the presence of a large number of interacting resonances, the physical scenario described by Eq. (14) is rather complicated and, in most cases, the minima of the scattering intensity must be retrieved by numerical methods. However, it is possible to precisely characterize the mutual interaction between external and internal modes in the case of isolated resonances, i.e. by assuming that the frequency spacing internal resonances is much larger than the damping factors $\mathbf{\Gamma}(\omega)$. Under these conditions, the scattering coefficients $\sigma_n^-(\omega)$ assume the familiar form:

$$\sigma_n^-(\omega) = \sum_m \lambda \frac{j(\omega-\omega_m)\left(e^{j\phi_n(\omega)}-1\right) - \Gamma_m\left(e^{j\phi_n(\omega)}+1\right)}{j(\omega-\omega_m)+\Gamma_m(\omega)}, \tag{15}$$

where we assumed that all the internal resonances interact only with one external eigenmode (see Supplementary Information). Equation (15) describe a scattering coefficient composed of several Fano-shaped profiles, which represent the characteristic signature of the interaction among localized resonances and a slowly-varying background [34, 32]. In Fig. (2)-a we report the scattering intensity in the proximity of a resonance placed at $\omega = \omega_m$, as a function of the normalized frequency $\tilde{\omega} = (\omega - \omega_m)/\Gamma_m$ and of the Fano coefficient $\phi_n(\omega)$. As can be seen from the figure, the final shape of the scattering spectrum is dictated by the value of the Fano parameter $\phi_n(\omega)$. If the external modes do not produce any reflection on the resonator boundary, i.e. $\phi_n = 0$, the scattering efficiency is characterized by a Lorentzian profile of width Γ_m and centered at $\omega = \omega_m$ (Fig. 2-b). Under these conditions, it is not possible to identify a specific scattering suppression condition. On the contrary, when the interaction between internal and external modes give rise to perfect reflection, corresponding to $\phi_n = \pi$, the scattering spectrum is characterized by a Lorentzian dip at $\omega = \omega_m$ (Fig. 2-d). In this configuration, the scattering suppression condition coincides with the internal resonance frequency. In the intermediate regime, where $0 < \phi_n(\omega) < \pi$, the scattering spectrum is characterized by a Fano-shaped profile (Fig. 2-c), with a strong scattering suppression condition corresponding to:

$$\omega_{anapole} = \omega_m - j\Gamma_m \frac{e^{j\phi_n(\omega)} + 1}{e^{j\phi_n(\omega)} - 1}. \tag{16}$$

In the next section we illustrate specific examples where the competition of different resonances lead to the formation of anapole states composed of different internal and external modes.

3.2. Fundamental and high-order anapoles in a dielectric disc

We apply the Fano-Feshbach projection developed in the previous section to investigate the formation of anapole states in circular two-dimensional cavities of radius R and dielectric function $\varepsilon(\mathbf{x}) = n^2$. The choice of such geometry is dictated by the fact that z-invariant cylindrical resonators can be easily fabricated, allowing for a convenient experimental observation of the anapole states [8]. As an input condition, we considered an incident plane wave directed along the x direction. In the closed cavity limit, the external eigenmodes can be obtained by solving Eq. (3) in the external space, obtaining:

$$|\nu_m(\mathbf{x}, \omega)\rangle = \sqrt{\frac{k}{8\pi}} \left[H_m^{(1)}(k\rho) - R_m^0(kR) H_n^{(2)}(k\rho) \right] e^{jm\phi}, \tag{17}$$

where $H^{(1,2)}$ are Hankel functions of the first and second type, respectively, and $R^0 = -\partial_\rho H^1(k\rho)/\partial_\rho H^2(k\rho)\big|_{\rho=R}$ was obtained by means of Eq. (4). As can be easily verified, such set of external eigenmodes correspond to the electromagnetic field produced by a TM-polarized plane wave impinging on a perfect electric conductor cylinder. In this context, the perfect conductor condition represents the electromagnetic equivalent of the closed cavity limit, with no radiation entering the cavity space, and all energy reflected at its boundary. The internal eigenmodes are obtained by solving the Helmholtz equation (3) in the resonator space, obtaining:

$$|\mu_{ml}\rangle = \frac{e^{jm\theta} J_m(nk_{ml}\rho)}{\sqrt{\pi} n R J_{m+1}(x_{ml})}, \tag{18}$$

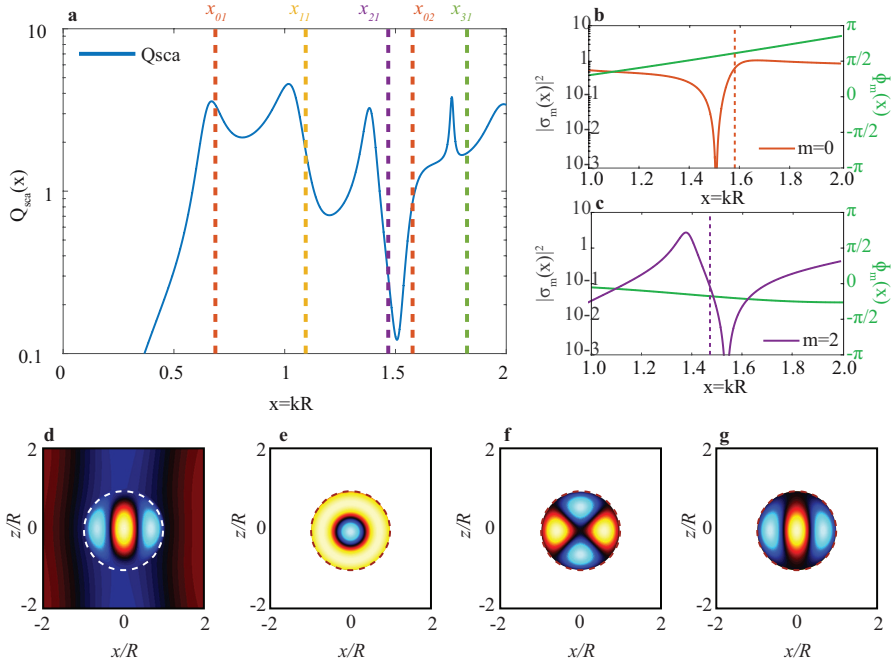

Figure 3. Anapole states in a silicon resonator (n=3.5). a Total scattering efficiency $Q_{sca}(x)$ and internal resonances (dotted vertical lines) as computed from the Fano-Feshbach partitioning scheme. The anapole state occurring at $x = 1.595$ can be explained as a superposition between the μ_{21} and μ_{02} modes. **b-c** Partial scattering intensity $|\sigma_m(x)|^2$ and Fano coefficient $\phi_m(x)$ for (b) m=0 and (c) m=2. **d** Electric field distribution of the Anapole state as computed from Lorentz-Mie theory. **e-f** Spatial distributions of the μ_{21} (e) and μ_{02} (f) resonances as computed with the Fano-Feshbach formalism. Their superposition (g) is in excellent agreement with the exact case.

where the internal resonance frequencies $x_{ml} = k_{ml}R$ coincide with the l-th zero of the Bessel function $J_m(\rho)$. In analogy with the angular momentum formalism, we introduced an additional discrete index l, which distinguishes the eigenmodes with the same order m but different number of zeros [40].

As a first example, we considered the scattering from a disc of silicon ($n = 3.5$) with radius of $R = 150$nm (Fig. 3). In Fig. 3-a, we report the Mie-Lorentz total scattering efficiency $Q_{sca}(x)$ as a function of the size parameter $x = kR$, being k the wavenumber of the incident plane wave. The vertical dotted lines correspond to the internal resonances x_{ml} as computed from Eq. (18). Even for such a simple geometry, it is possible to easily identify an anapole state at $x = 1.525$ (see Fig. 3-a), whose electric field distribution is reported in Fig. 4-a (cfr. Fig. 3 of [9] and Fig. 5 of [18]). The Fano-Feschbach partitioning unveils the presence of two distinct resonances generating the anapole state: a first one, corresponding to the cavity mode $|\mu_{02}\rangle$, with $m = 0$ and $l = 2$ and a higher order mode with $m = 2$ and $l = 1$ (Fig. 3-e,f). These resonances are coupled to different external channels and, therefore, they are mutually independent, provided that as the coupling amplitudes $\Gamma_{mll'}$ connect only states with the same angular momentum index $m' = m$. However, both these resonances are individually characterized by Fano-shaped profiles, as it

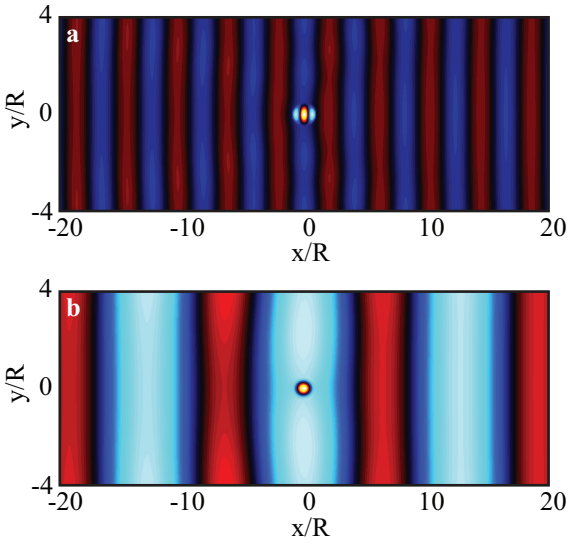

Figure 4. Scattering suppression in anapole states Electric field distribution and scattering suppression in a silicon resonator (a, n=3.5, x=1.595) and in a high-refractive index resonator (b, n=8, x=0.495).

can be evinced by inspecting their scattering response separately (Fig. 3-b,c). The $m = 0$ mode, which is characterized by a large and positive Fano parameter ϕ_0 in the proximity of the resonance (Fig. 3-b, green line), provides for a quasi-lorentzian dip (Fig. 3-b, orange line). The $m = 2$ mode, conversely, presents a small and negative Fano parameter (Fig. 3-c, green line) yielding an almost symmetric Fano profile (Fig. 3-c, violet line). When these resonances are placed in the proximity of each other, their superposition produces a strong cancellation of the total scattering efficiency. As a further confirmation that the anapole state is generated by the superposition of two distinct resonances, we compare the exact electric field distribution computed from Lorentz-Mie theory (Fig. 3-d) with the internal modes distribution for the two resonances (Fig. 3-e,f). Remarkably, their superposition (Fig. 3-g), as computed from the Fano-Feshbach approach, is in strongly agreement with the exact solution from Maxwell's equations. Interestingly, the fundamental anapole state at $x = 1.525$ is the only scattering reduction state for this geometry, as in a two-dimensional structure higher-order anapole states are suppressed by the strong scattering from nearby resonances [8, 41]. As a result, no additional anapole states can be identified for larger values of x (see Supplementary Figure 1).

By increasing the refractive index of the resonator, it is possible to identify even more complex scenarios, as reported in Fig. 5, where we considered a dielectric disc with the same geometry but refractive index $n = 8$. Such high value for the refractive index can be easily obtained in experiments by considering, e.g., the refractive index of water in the microwave spectrum [8]. As it can be observed from the total scattering efficiency (Fig. 5-a), in the case of a high-index nanoparticle the resonances are much narrower and closer, producing a complicated Mie scattering profile characterized by distinct Fano-shaped profiles. As a result, it is possible to identify three anapole states, occurring at $x = 0.49$, $x = 1.495$ and $x = 1.896$, respectively (Fig. 5-a, gray bars). Such states are the result of the competition of multiple Fabo-Feshbach resonances:

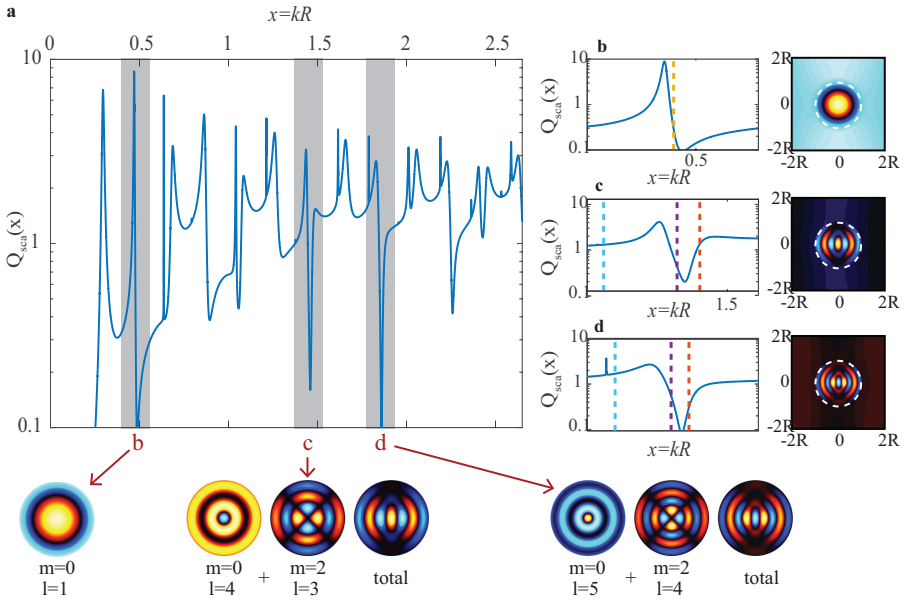

Figure 5. Higher order anapole states in a a high-index resonator (n=8). **a** Total scattering efficiency $Q_{sca}(x)$. Three invisibility states can be identified (gray areas), which can be interpreted in terms of different superpositions of internal modes (inset). **b, d** As in the silicon case, the invisibility states are characterized by different superposition of internal and external channels. While in the first state at $x = 0.495$ (b) the invisibility is due to a pure state ($m = 0, l = 1$), in the higher order invisibility modes the internal modes are characterized by the superposition of two different internal modes, with $m = 0$ and $m = 2$ and different values of l (c,d).

in the first case ($x = 0.49$, cfr. Fig. 5-b), the invisibility state is due to the excitation of a single internal mode μ_{01}, with $m = 0, l = 1$ mode (yellow dashed line). The higher order anapole states, conversely, are characterized by the mutual interaction between states with $m = 0$ (orange dashed lines), and $m = 2$ (violet dashed lines) with different values of l(Fig. 5-c,d). As in the case of the silicon resonator, we computed the spatial distributions for the internal modes responsible for the anapole state formation. Their superposition (Fig. 5-a, inset) is in very good agreement with the results from Lorentz-Mie theory (insets of Fig. 5-b,d). These additional Anapole states, unvelied by this theoretical Fano-Feshbach description, cannot be represented in terms of fundamental anapole modes, and they have been experimentally observed in Germanium nanoparticles [18]. An interesting question is whether it is possible to express these states in terms of high-order toroidal dipoles [10]. This question, which is clearly beyond the scope of this paper, is a current topic of investigation [10, 42], and it will be addressed in a future separate work on the subject.

4. Conclusions

We investigated the generation of anapole states in generic dielectric nanostructures by introducing a Fano-Feshbach projection technique, which represents a fundamental tool for the investigation of resonant phenomena in open systems. Differently from previous approaches, aiming at the quantization of the electromagnetic field, we expanded the electric field $\mathbf{E}(\mathbf{x}, t)$ into two orthogonal sets of internal and external eigenmodes, which are mutually coupled by *ad hoc* boundary terms. Additionally, we addressed the definition of a complete electromagnetic scattering problem, obtaining a general expression for the scattered field as generated by a known incident field. As an illustrative example of the Fano-Feshbach partitioning tehcnique, we investigated the formation of Anapole states in a circular dielectric cavity, which constitutes a geometry which can be fabricated with standard techniques. Our results show that even such simple resonator structures support the formation of high-order anapoles, originated from the superposition of several internal modes, which we completely identify and characterize by means of the Fano-Feshbach approach.

References

[1] Francesco Monticone and Andrea Alù. Invisibility exposed: physical bounds on passive cloaking. *Optica*, 3(7):718, July 2016.

[2] Ken Xingze Wang, Zongfu Yu, Sunil Sandhu, Victor Liu, and Shanhui Fan. Condition for perfect antireflection by optical resonance at material interface. *Optica*, 1(6):388, December 2014.

[3] S. Feng, K. Halterman, P. L. Overfelt, J. M. Elson, G. A. Lindsay, and M. J. Roberts. Resonant-induced transparency and coupled modes in layered metamaterials. *Applied Physics A*, 87(2):235–244, February 2007.

[4] KB Samusev, MV Rybin, AK Samusev, and MF Limonov. Invisibility of a finite dielectric cylinder under fano resonance conditions. *Physics of the Solid State*, 57(10):1991–1996, 2015.

[5] Xiaodong Yang, Mingbin Yu, Dim-Lee Kwong, and Chee Wei Wong. All-Optical Analog to Electromagnetically Induced Transparency in Multiple Coupled Photonic Crystal Cavities. *Physical Review Letters*, 102(17):173902, April 2009.

[6] Pengyu Fan, Uday K. Chettiar, Linyou Cao, Farzaneh Afshinmanesh, Nader Engheta, and Mark L. Brongersma. An invisible metal-semiconductor photodetector. *Nature Photonics*, 6(6):380–385, June 2012.

[7] Pai-Yen Chen, Jason Soric, and Andrea Alù. Invisibility and Cloaking Based on Scattering Cancellation. *Advanced Materials*, 24(44):OP281–OP304, November 2012.

[8] Mikhail V. Rybin, Dmitry S. Filonov, Pavel A. Belov, Yuri S. Kivshar, and Mikhail F. Limonov. Switching from Visibility to Invisibility via Fano Resonances: Theory and Experiment. *Scientific Reports*, 5:8774, March 2015.

[9] Andrey E. Miroshnichenko, Andrey B. Evlyukhin, Ye Feng Yu, Reuben M. Bakker, Arkadi Chipouline, Arseniy I. Kuznetsov, Boris Luk'yanchuk, Boris N. Chichkov, and Yuri S. Kivshar. Nonradiating anapole modes in dielectric nanoparticles. *Nature Communications*, 6:8069, August 2015.

[10] Stefan Nanz. *Toroidal Multipole Moments in Classical Electrodynamics*. Springer Fachmedien Wiesbaden, Wiesbaden, 2016.

[11] V. M. Dubovik and V. V. Tugushev. Toroid moments in electrodynamics and solid-state physics. *Physics Reports*, 187(4):145–202, March 1990.

[12] T. Kaelberer, V. A. Fedotov, N. Papasimakis, D. P. Tsai, and N. I. Zheludev. Toroidal Dipolar Response in a Metamaterial. *Science*, 330(6010):1510–1512, December 2010.

[13] Chiu Man Ho and Robert J. Scherrer. Anapole dark matter. *Physics Letters B*, 722(4–5):341–346, May 2013.

[14] Wei Liu, Jianfa Zhang, Bing Lei, Haojun Hu, and Andrey E. Miroshnichenko. Invisible nanowires with interfering electric and toroidal dipoles. *Optics Letters*, 40(10):2293, May 2015.

[15] Wei Liu, Jianfa Zhang, and Andrey E. Miroshnichenko. Toroidal dipole induced transparency for core-shell nanoparticles. *Laser & Photonics Reviews*, 9(5):564–570, September 2015. arXiv: 1412.4931.

[16] Lei Wei, Zheng Xi, Nandini Bhattacharya, and H. Paul Urbach. Excitation of the radiationless anapole mode. *Optica*, 3(8):799, August 2016.

[17] Gustavo Grinblat, Yi Li, Michael P. Nielsen, Rupert F. Oulton, and Stefan A. Maier. Enhanced Third Harmonic Generation in Single Germanium Nanodisks Excited at the Anapole Mode. *Nano Letters*, June 2016.

[18] Gustavo Grinblat, Yi Li, Michael P Nielsen, Rupert F Oulton, and Stefan A. Maier. Efficient Third Harmonic Generation and Nonlinear Sub-Wavelength Imaging at a Higher-Order Anapole Mode in a Single Germanium Nanodisk. *ACS Nano*, December 2016.

[19] F. Antenucci, C. Conti, A. Crisanti, and L. Leuzzi. General Phase Diagram of Multimodal Ordered and Disordered Lasers in Closed and Open Cavities. *Physical Review Letters*, 114(4):043901, January 2015.

[20] Philip Trøst Kristensen and Stephen Hughes. Modes and Mode Volumes of Leaky Optical Cavities and Plasmonic Nanoresonators. *ACS Photonics*, 1(1):2–10, January 2014.

[21] Hakan E. Türeci, A. Douglas Stone, and B. Collier. Self-consistent multimode lasing theory for complex or random lasing media. *Physical Review A*, 74(4):043822, October 2006.

[22] Carlos Viviescas and Gregor Hackenbroich. Field quantization for open optical cavities. *Physical Review A*, 67(1):013805, January 2003.

[23] Changxu Liu, Ruben EC Van Der Wel, Nir Rotenberg, L Kuipers, Thomas Fraser Krauss, Andrea Di Falco, and Andrea Fratalocchi. Triggering extreme events at the nanoscale in photonic seas. *Nature Physics*, 11(4):358–363, 2015.

[24] Roman Bruck, Changxu Liu, Otto L Muskens, Andrea Fratalocchi, and Andrea Falco. Ultrafast all-optical order-to-chaos transition in silicon photonic crystal chips. *Laser & Photonics Reviews*, 2016.

[25] Juan Sebastian Totero Gongora and Andrea Fratalocchi. Harnessing Disorder at the Nanoscale. In Bharat Bhushan, editor, *Encyclopedia of Nanotechnology*, pages 1–13. Springer Netherlands, 2015. DOI: 10.1007/978-94-007-6178-0_101015-1.

[26] Andrey E. Miroshnichenko, Sergej Flach, and Yuri S. Kivshar. Fano resonances in nanoscale structures. *Reviews of Modern Physics*, 82(3):2257–2298, August 2010.

[27] Philip McCord Morse and Herman Feshbach. *Methods of theoretical physics*. McGraw-Hill, 1953.

[28] Cheng Chin, Rudolf Grimm, Paul Julienne, and Eite Tiesinga. Feshbach resonances in ultracold gases. *Reviews of Modern Physics*, 82(2):1225–1286, April 2010.

[29] Herman Feshbach. Unified theory of nuclear reactions. *Annals of Physics*, 5(4):357–390, December 1958.

[30] U. Fano. Effects of Configuration Interaction on Intensities and Phase Shifts. *Physical Review*, 124(6):1866–1878, December 1961.

[31] Dariusz Chruściński and Andrzej Kossakowski. Feshbach Projection Formalism for Open Quantum Systems. *Physical Review Letters*, 111(5):050402, July 2013.

[32] Shanhui Fan, Wonjoo Suh, and J. D. Joannopoulos. Temporal coupled-mode theory for the Fano resonance in optical resonators. *Journal of the Optical Society of America A*, 20(3):569, 2003.

[33] Zhichao Ruan and Shanhui Fan. Superscattering of Light from Subwavelength Nanostructures. *Physical Review Letters*, 105(1):013901, June 2010.

[34] Zhichao Ruan and Shanhui Fan. Temporal Coupled-Mode Theory for Fano Resonance in Light Scattering by a Single Obstacle . *The Journal of Physical Chemistry C*, 114(16):7324–7329, April 2010.

[35] Zhichao Ruan and Shanhui Fan. Temporal coupled-mode theory for light scattering by an arbitrarily shaped object supporting a single resonance. *Physical Review A*, 85(4), April 2012.

[36] David Pile. Coupled-mode theory: Time-dependence. *Nature Photonics*, 6(7):412–412, July 2012.

[37] Vladislav Shteeman and Amos A. Hardy. Analysis of advanced photonic devices with time-dependent coupled mode equations. *Optical Engineering*, 51(5):054001–1, 2012.

[38] Juan Sebastian Totero Gongora, Andrey E Miroshnichenko, Yuri S Kivshar, and Andrea Fratalocchi. Energy equipartition and unidirectional emission in a spaser nanolaser. *Laser & Photonics Reviews*, 10(3):432–440, 2016.

[39] Craig F Bohren and Donald R Huffman. *Absorption and scattering of light by small particles*. John Wiley & Sons, 2008.

[40] C. Viviescas and G. Hackenbroich. Quantum theory of multimode fields: applications to optical resonators. *Journal of Optics B: Quantum and Semiclassical Optics*, 6(4):211, April 2004.

[41] Michael I. Tribelsky and Andrey E. Miroshnichenko. Giant in-particle field concentration and Fano resonances at light scattering by high-refractive-index particles. *Physical Review A*,

93(5), May 2016.

[42] Wu-Chao Zhai, Tie-Zhu Qiao, Dong-Jin Cai, Wen-Jie Wang, Jing-Dong Chen, Zhi-Hui Chen, and Shao-Ding Liu. Anticrossing double Fano resonances generated in metallic/dielectric hybrid nanostructures using nonradiative anapole modes for enhanced nonlinear optical effects. *Optics Express*, 24(24):27858–27869, November 2016.